

Longitudinal relaxation and thermoactivation of quantum superparamagnets

D. Zueco and J. L. García-Palacios

Departamento de Física de la Materia Condensada e Instituto de Ciencia de Materiales de Aragón, C.S.I.C., Universidad de Zaragoza, E-50009 Zaragoza, Spain

(Received 27 September 2005; revised manuscript received 10 January 2006; published 30 March 2006)

The relaxation mechanisms of a quantum nanomagnet are discussed in the framework of linear response theory. We use a spin Hamiltonian with a uniaxial potential barrier plus a Zeeman term. The spin, having arbitrary S , is coupled to a bosonic environment (phonons). From the eigenstructure of the relaxation matrix, we identify two main mechanisms: namely, thermal activation over the barrier, with a time scale Λ_1^{-1} , and a faster dynamics inside the potential wells, with characteristic time Λ_w^{-1} . This permits to introduce a simple analytical formula for the response, which agrees well with exact numerical results and covers experiments even under moderate to strong fields in the superparamagnetic range. In passing, we generalize known classical results for a number of quantities (e.g., integral relaxation times, initial decay time, Kramers' rate), results that are recovered in the limit $S \rightarrow \infty$.

DOI: [10.1103/PhysRevB.73.104448](https://doi.org/10.1103/PhysRevB.73.104448)

PACS number(s): 75.50.Xx, 75.50.Tt, 03.65.Yz, 05.40.-a

I. INTRODUCTION

Superparamagnets are nanoscale magnetic solids or clusters effectively described in terms of their net spin. They have an internal anisotropy barrier with several local equilibrium states. The spin is coupled to the environmental degrees of freedom of the host material (phonons, nuclear spins, electrons, etc.). This interaction provokes dynamical disturbances on the spin, which can “jump” over the barrier separating the potential minima, giving rise to the phenomenon of *superparamagnetism*. The prefix *super* stems from the typically large net spins of these systems ($S \sim 10^1 - 10^4$).

Single-domain magnetic particles are an example of such nanoscale solids, having a magnetic moment of a few thousand Bohr magnetons.¹ Due to their enormous spin, these particles can be described classically.^{2,3} Another example is provided by single-molecule magnets, such as Mn_{12} , Fe_8 , or Ni_{12} .⁴ Their net spin is $S \sim 10$, so that the classical description is no longer valid and a quantum treatment is required. Still, these molecules comprise a few hundreds of atoms, yielding an interplay of quantumness and mesoscopicity that has stimulated an intense research in recent years.

Classically, the spin surmounts the barrier ΔU by thermal activation. When $\Delta U/k_B T \gg 1$ the characteristic time for this overbarrier process can be written in Arrhenius' form $\tau \equiv \Lambda_1^{-1} \propto \exp(\Delta U/k_B T)$. This is the rotational counterpart of the Kramers' rate in the theory of activated processes in translational systems.^{5,6} The classical dynamics of these systems has been studied extensively. The transverse response (i.e., perpendicular to the anisotropy axis) is nearly constant (except at ferromagnetic resonance frequencies) and equals the thermal equilibrium response. More interesting is the *longitudinal* response; its analysis revealed that an one-mode relaxation picture with time scale Λ_1^{-1} is not valid in general.^{7,8} A satisfactory description, however, is provided by a two-mode response, one mode corresponding to the overbarrier flux and the other, with a characteristic scale Λ_w^{-1} , describing the faster intrawell dynamics.⁹

Quantum mechanically, spin reversal can take place by thermal activation or tunneling (or a combination of

both).¹⁰⁻¹⁶ Tunneling may occur from one side of the barrier to the other (Fig. 1) between resonant, equal-energy states “coupled” by transverse fields (or high-order anisotropy terms). However, as in any quantum-mechanical problem, the tunnel splitting (and hence its probability) decreases exponentially from the maxima down to the potential wells (in Mn_{12} tunneling is effective only through a few states near the barrier top, $|m| \leq 3, 4$). Thus, in the superparamagnetic regime ($T \geq 2$ K) thermal activation governs the physics: (i) out of resonance, the transitions can only be driven by thermal activation, while (ii) tunneling in resonance results in a lowering of the effective barrier by a few states [$\Delta U = (\epsilon_0 - \epsilon_{\pm S}) \rightarrow (\epsilon_{3,4} - \epsilon_{\pm S})$].

The theory of quantum thermal activation has focused mainly on the zero- or very-weak-field limit.^{17,18} Then the relaxation becomes well described by one mode—the overbarrier process. The effect of bias fields, beyond the weak-field regime, has been studied only on the thermoactivation rate,¹⁹ but not on the susceptibility. Thus studies of the full dynamical response including the effect of applied fields are demanded. This is the issue we address in this work: the

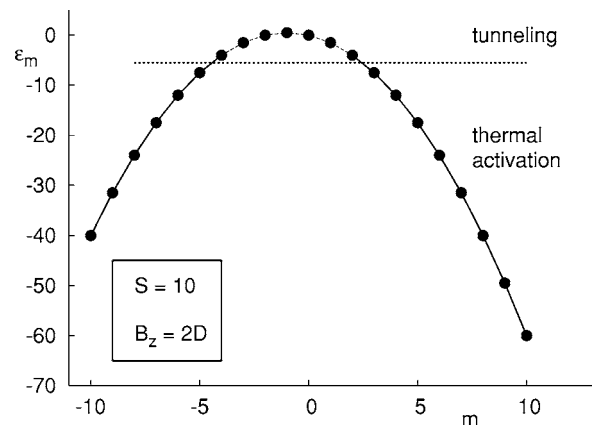


FIG. 1. Energy levels of a moderate spin described by Hamiltonian (1) with $D=0.5$ at $B_z=1$. Considering D in kelvin, the values given correspond closely to those of Mn_{12} .

relaxation of a spin with arbitrary S in contact with a bosonic (phonon) environment. The dynamics is studied in the framework of quantum master (balance) equations with help from linear-response-theory tools. We concentrate on the case of longitudinal applied fields, giving a complete characterization of the relaxation mechanisms. The connection with the classical theory is done taking the $S \rightarrow \infty$ limit (whenever well defined) recovering known classical results.

The paper is organized as follows. In Sec. II we present the quantum balance equations. The tools of linear-response theory employed are discussed in Sec. III as well as the eigenstructure of the relaxation matrix. Its eigenvalue spectrum suggest the introduction of a two-mode description of the susceptibility (Sec. IV) following closely the approach of Kalmykov and co-workers in the classical limit.⁹ The comparison between exact numerical results and such an analytical approximation is done in Sec. V. We give a full physical interpretation of the results obtained and present also simplified expressions (for both the susceptibility and relaxation times), in the Kramers' range $\Delta U/k_B T \gtrsim 10-20$, experimentally the most relevant for superparamagnets. Technical details of some calculations are relegated to the appendixes.

II. RELAXATION OF A QUANTUM SPIN

A. Spin Hamiltonian and balance equations

The minimal Hamiltonian capturing the physics of superparamagnets includes a uniaxial anisotropy term plus the Zeeman coupling with external fields.²⁰ Here we study the longitudinal relaxation in the presence of fields parallel to the anisotropy axis ($\hbar = g\mu_B = k_B = 1$):

$$\mathcal{H} = -DS_z^2 - B_z S_z. \quad (1)$$

In the standard basis $S_z|m\rangle = m|m\rangle$, this Hamiltonian exhibits a spectrum ε_m with a double-well structure and minima at $m = \pm S$ [for $B_z < D(2S-1)$; see Fig. 1]. The barrier heights are $\Delta U_{\pm} = \varepsilon_{m_b} - \varepsilon_{\pm S}$, where m_b is the index corresponding to the maximum level.²¹ For fields $B_z \gtrsim D(2S-1)$ the barrier disappears and the spectrum approaches the custom equispaced Zeeman spectrum $\varepsilon_m \approx -B_z m$ for $B_z/2D \gg S$.

The relaxation induced by the spin environment is typically described by a set of *balance equations* for the diagonal terms of the density matrix ρ (Ref. 22):

$$\dot{N}_m = (P_{m|m+1}N_{m+1} - P_{m+1|m}N_m) + (P_{m|m-1}N_{m-1} - P_{m-1|m}N_m), \quad (2)$$

where $N_m \equiv \rho_{mm} = \langle m|\rho|m\rangle$ are the level populations. The transition probabilities $P_{m|m'}$ depend on the energy differences $\Delta_{mm'} \equiv \varepsilon_m - \varepsilon_{m'}$. They fulfill the detailed balance condition

$$P_{m|m'} = e^{-\beta\Delta_{mm'}} P_{m'|m}, \quad (3)$$

which ensures that the Gibbs distribution $N_m^{(0)} = e^{-\beta\varepsilon_m}/\mathcal{Z}$ is a stationary solution of Eq. (2) ($\dot{N}_m = 0$).

B. Spin plus bath formulation

The balance equations can be obtained in a phenomenological way: postulating the form (2) and then calculating the

probabilities $P_{m|m'}$ by means of Fermi's golden rule.²³ They can also be obtained in a more rigorous way.^{14,19,24} One starts from a total Hamiltonian representing the spin and its environment:

$$\mathcal{H}_{\text{tot}} = \mathcal{H}(S) + \sum_q V_q F_q(S) (a_q^\dagger + a_{-q}) + \mathcal{H}_B. \quad (4)$$

Here $\mathcal{H}_B = \sum_q \omega_q a_q^\dagger a_{-q}$ is a bosonic bath modeling the excitations of the host material, $F_q(S)$ the spin-dependent part of the interaction, and V_q coupling constants. If the spin-bath coupling is weak, the equation of motion for the density matrix ρ can be obtained within perturbation theory. After the secular (rotating-wave) approximation and in the absence of transverse fields, the equations for each (sub)diagonal of the density matrix, $\rho_{m,m+k}$, become uncoupled from one another.²⁵ In particular the populations ρ_{mm} form a closed set of kinetic equations, like Eq. (2).^{26,27}

In this frame, the transition probabilities are given by

$$P_{m|m'} = |\bar{\ell}_{m,m'}|^2 W_{m|m'}, \quad (5)$$

where $\bar{\ell}_{m,m'}$ are the matrix elements of the spin-dependent part of the coupling $F(S)$. When the spectral density of the bath, $J(\omega) \equiv \pi \sum_q |V_q|^2 \delta(\omega - \omega_q)$, has the form $J = \lambda \omega^\kappa$ (λ is a spin-bath coupling strength), the rates $W_{m|m'} \equiv W(\Delta_{mm'})$ are given by the following universal function:

$$W(\Delta) = \frac{\lambda \Delta^\kappa}{e^{\beta\Delta} - 1}. \quad (6)$$

When $\kappa=1$, the bath is *Ohmic*, while if $\kappa>1$, it is called *super-Ohmic*.^{28,29}

Having molecular magnets in mind, we will consider a super-Ohmic bath ($\kappa=3$) and the coupling $F(S) \propto (S_z S_\pm + S_\pm S_z)$, for which $\bar{\ell}_{m,m\pm 1} = (2m \pm 1) \sqrt{S(S+1) - m(m \pm 1)}$.^{13,14,25} This models the interaction with three-dimensional (3D) phonons including one-phonon emission and absorption processes, the relevant ones at low temperatures.³⁰ The modifications required to include other structures of the coupling, or other baths, would only involve the $P_{m|m'}$ and are easy to carry out.

C. Classical limit

As we would like to make the connection of our calculations with known results for classical superparamagnets, let us briefly consider the $S \rightarrow \infty$ limit of the balance equations (2). To this end we introduce the scaled anisotropy and field parameters:

$$\sigma \equiv \beta D S^2, \quad \xi \equiv \beta B_z S, \quad h \equiv \frac{\xi}{(2-1/S)\sigma}. \quad (7)$$

Then the scaled Hamiltonian reads $\beta\mathcal{H} = -\sigma(m/S)^2 - \xi(m/S)$. The first two quantities σ and ξ are equivalent to those used in the description of magnetic nanoparticles.⁷⁻⁹ The "reduced field" h is B_z measured in terms of the field for barrier disappearance $D(2S-1)$; it differs from the usual classical definition $h_{\text{cl}} = \xi/(2\sigma)$ due to the discreteness of the energy levels.

The quantities σ and ξ are kept constant when taking the limit $S \rightarrow \infty$. Then $m/S \rightarrow z$, while $h \rightarrow h_{cl}$ and $\beta\mathcal{H} \rightarrow -\sigma z^2 - \xi z \equiv u(z)$. Physically more and more levels are introduced, towards a continuum, while keeping the anisotropy barrier and amount of Zeeman energy constant. In this limit the transition frequencies $\Delta_{m,m\pm 1}$ tend to zero. Then, no relaxation is left in the classical case if $P_{m|m\pm 1}(0)=0$. Such is the case for a pure super-Ohmic environment. A well-defined classical limit is obtained for an *Ohmic* bath, such as, for instance, in the Kondo coupling to electron-hole excitations.²⁹ Besides, just adding two-phonon (Raman) processes in the interaction to phonons one gets $P_{m|m\pm 1}(0) \neq 0$ too. In these cases, the balance equations (2) go in the limit $S \rightarrow \infty$ over a partial differential equation

$$\frac{\partial W}{\partial t} = \frac{\partial}{\partial z} \left[G(z) \left(\frac{\partial W}{\partial z} + \frac{\partial u}{\partial z} W \right) \right], \quad (8)$$

with $W(z,t)$ the probability distribution of z and $P_{m+1|m}(0)/S^2 \rightarrow G(z)$ (see Appendix A for the details). For $G(z) \propto (1-z^2)$, Eq. (8) corresponds to Brown's *Fokker-Planck* equation for classical superparamagnets in the absence of transverse field³ and to the rotational kinetic equations used in dielectric relaxation.³¹

III. ANALYSIS OF THE LONGITUDINAL RESPONSE

The purpose of this section is to present the theoretical tools necessary to describe the spin relaxation. To made a system to "relax" we must put it first in a nonequilibrium situation (e.g., subjecting it to a perturbation in the external field). The response to this probe informs about the relaxation mechanisms of the system. We will use linear-response-theory tools³² and the analysis of the eigenstructure of the balance equations.²⁴

Equation (2) is indeed a set of linear differential equations for the level populations N_m . In matrix form it can be written as $d\mathbf{N}/dt = -\mathcal{R}\mathbf{N}$, with $[\mathbf{N}]_m \equiv N_m$ and \mathcal{R} the *relaxation matrix*. We assume \mathcal{R} diagonalizable and express the solution for N_m as

$$\mathbf{N} = \sum_{i=1}^{2S} c_i e^{-\Lambda_i t} |\Lambda_i\rangle + |\Lambda_0\rangle, \quad [\mathbf{N}]_m = N_m, \quad (9)$$

with Λ_i the eigenvalues of \mathcal{R} and $|\Lambda_i\rangle$ the associated eigenvectors.³³ The last term in Eq. (9) corresponds to the equilibrium solution—i.e., $|\Lambda_0\rangle_m \equiv N_m^{(0)} \propto e^{-\beta \varepsilon_m}$. The relaxation matrix \mathcal{R} must give $\text{Re}(\Lambda_i) > 0$, ensuring that the asymptotic solution will be the equilibrium one.²⁴

A. Linear response theory

For the effect of an applied perturbation to reflect the *intrinsic* properties of the system the force should be suitably small. The weakness of the probe has the technical advantage of allowing one to use linear-response theory. Several "experiments" can be made to study the response: namely, subjecting the system to a sudden constant "force" or by removing a force after having kept it on for a long time. One can also consider the response to a force oscillating with fre-

quency Ω . Linear-response theory provides the close relationship between these types of responses.

Assume first that we have excited the spin system with a constant field δB_z , keeping it on until the system is equilibrated (in a total field $B_z^0 + \delta B_z$). Then, we switch the perturbation off and measure the response:

$$\Delta M_z(t) \equiv \langle M_z(t) \rangle - \langle M_z \rangle_0. \quad (10)$$

Here $\langle M_z \rangle_0$ is the statistical average at equilibrium with $B_z = B_z^0$ and $\langle M_z(t) \rangle = \sum_m m N_m(t)$. Since the asymptotic solution for the N_m is the equilibrium one in $B_z = B_z^0$, then $\langle M_z \rangle_0 = \langle M_z(t \rightarrow \infty) \rangle$. Indeed, introducing the solution (9) for $N_m(t)$ in $\langle M_z(t) \rangle$, we find

$$\Delta M_z = \chi_z \delta B_z \sum_{i=1}^{2S} a_i e^{-\Lambda_i t}, \quad (11)$$

where $\chi_z \equiv \partial \langle M_z \rangle_0 / \partial B_z$ is the equilibrium susceptibility. In linear response χ_z equals $[\langle M_z(0) \rangle - \langle M_z(\infty) \rangle] / \delta B_z$. The coefficients a_i are given in terms of the eigenvalues of the relaxation matrix \mathcal{R} and the coefficients c_i by [see Eq. (9)]:

$$a_i = \frac{\tilde{c}_i}{\chi_z} \sum_{m=-S}^S m |\Lambda_i\rangle_m. \quad (12)$$

Here c_i has been redefined as $\tilde{c}_i \equiv c_i / \delta B_z$, to get rid of dependences on δB_z . The coefficients a_i obey the normalization condition $\sum_{i=1}^{2S} a_i = 1$ which follows from the definition (12) and the equality $\chi_z = \sum_i \tilde{c}_i \sum_m m |\Lambda_i\rangle_m$. The \tilde{c}_i can be evaluated putting $t=0$ in Eq. (9). The initial condition is the system equilibrated at $B = B_z^0 + \delta B_z$. The occupation numbers can be written in linear approximation as $N_m(t=0) \equiv N_m^{(0)} B_z^0 + \delta B_z \partial_{B_z} N_m^{(0)}|_{B_z^0}$, so that the \tilde{c}_i 's obey

$$\frac{\partial N_m^{(0)}}{\partial B_z} \Big|_{B_z^0} = \sum_{i=1}^{2S} \tilde{c}_i |\Lambda_i\rangle_m, \quad (13)$$

which is an overdetermined set of $2S+1$ linear equations (there are $2S$ c_i 's). Both $|\Lambda_i\rangle$ and then \tilde{c}_i can be obtained using standard linear-algebra numerical routines.³⁴

Finally, let us consider the relation with the other relaxation experiments. The case with the system equilibrated at $B_z = B_z^0$ and a perturbation δB_z suddenly added is just the complementary situation to that discussed above. More interesting is the oscillating field probe. Here we define the dynamical susceptibility $\chi(\Omega)$ as the coefficient which relates (in the frequency domain) response and excitation: $\Delta M_z(\Omega) = \chi(\Omega) \delta B_z(\Omega)$ with $\tilde{g}(\Omega) = \int dt e^{-i\Omega t} g(t)$. Then the response to a periodic perturbation, $\delta B_z(t) \propto e^{-i\Omega t}$, is given by

$$\chi(\Omega) = \chi_z \left[1 - i\Omega \int_0^\infty dt \frac{\Delta M_z(t)}{\Delta M_z(0)} e^{-i\Omega t} \right] = \chi_z \sum_{i=1}^{2S} \frac{a_i}{1 + i\Omega \Lambda_i^{-1}}. \quad (14)$$

Equations (11) and (14) provide the relation between the different relaxation experiments. The analysis of the response gives the time scales Λ_i^{-1} and the weights a_i 's of the modes involved in the relaxation process. Note finally that

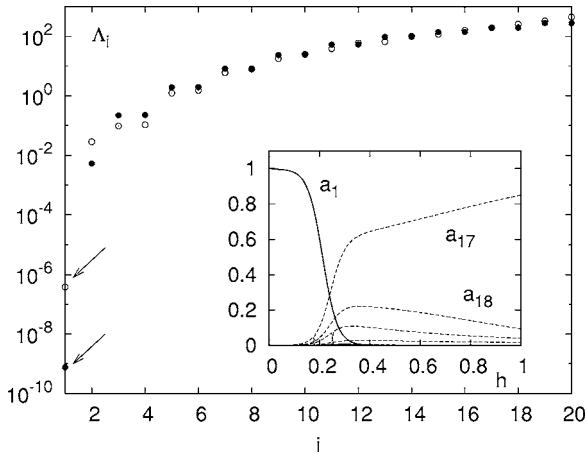


FIG. 2. Eigenvalues of the relaxation matrix \mathcal{R} for a spin $S = 10$ with $\sigma = \beta DS^2 = 15$ at zero field (solid symbols) and at $h = 0.2$ (open symbols, normalized by the spin-bath coupling $\lambda = 10^{-9}$). The arrows mark the lowest nonvanishing eigenvalue Λ_1 . Inset: field dependence of the coefficients a_i .

neither Λ_i nor a_i depends on the external probe but only on the intrinsic dynamics of the system, as was intended.

B. Eigenvalue and eigenvector structure

Attending at the evolution of \mathbf{N} in Eq. (9), we see that the eigenvectors of \mathcal{R} determine how the redistribution of the levels' populations occurs ($[\mathbf{N}]_m = N_m$), while the eigenvalues give the associated time scales Λ_i^{-1} . They can be obtained by numerical diagonalization of \mathcal{R} and are plotted, indexed in increasing order, in Figs. 2 and 3 for $S = 10$.

Apart from the zero eigenvalue (not plotted), the eigenvalues correspond to two, well-separated, sets of time scales (on the one side Λ_1 and $\Lambda_2 \rightarrow \Lambda_{2S}$ on the other). From the structure of the corresponding eigenvectors (Fig. 3) we see that the dynamics associated with $|\Lambda_1\rangle$ produces an increment in the population at the bottom of one well and depopulation at the other (or the other way around, since the global sign of the eigenvectors does not matter). Since this transfer occurs across the barrier, the mode $|\Lambda_1\rangle$ is associated to the overbarrier dynamics. On the other hand, $|\Lambda_2\rangle$ represents the transfer from $m = 0$ to both wells or vice versa (not changing the net population of the wells). Further, $|\Lambda_3\rangle$ and $|\Lambda_4\rangle$ account for dynamics involving $m = \pm 1$ and $m = \pm S$, respectively, and so on. Eventually $|\Lambda_{17}\rangle - |\Lambda_{20}\rangle$ ($20 = 2S$) involve the levels closer to the bottom of the wells. All these processes are called intrawell ones, since no activation over the barrier is involved. Thus the slow, and well-separated, time scale Λ_1^{-1} corresponds to the overbarrier dynamics, whereas the set of close (in logarithmic scale) intrawell processes is responsible for the fast dynamics.

Let us briefly comment on two aspects of the eigenstructure. First, apart from Λ_0 , Λ_1 , and Λ_2 , the remaining eigenvalues appear doubly degenerated (at $B_z = 0$).³⁵ Physically each member of the degenerate pair describes identical processes in different wells, and at zero field both wells are equivalent. When $B_z \neq 0$ the equivalence is broken and the degeneration lifted.

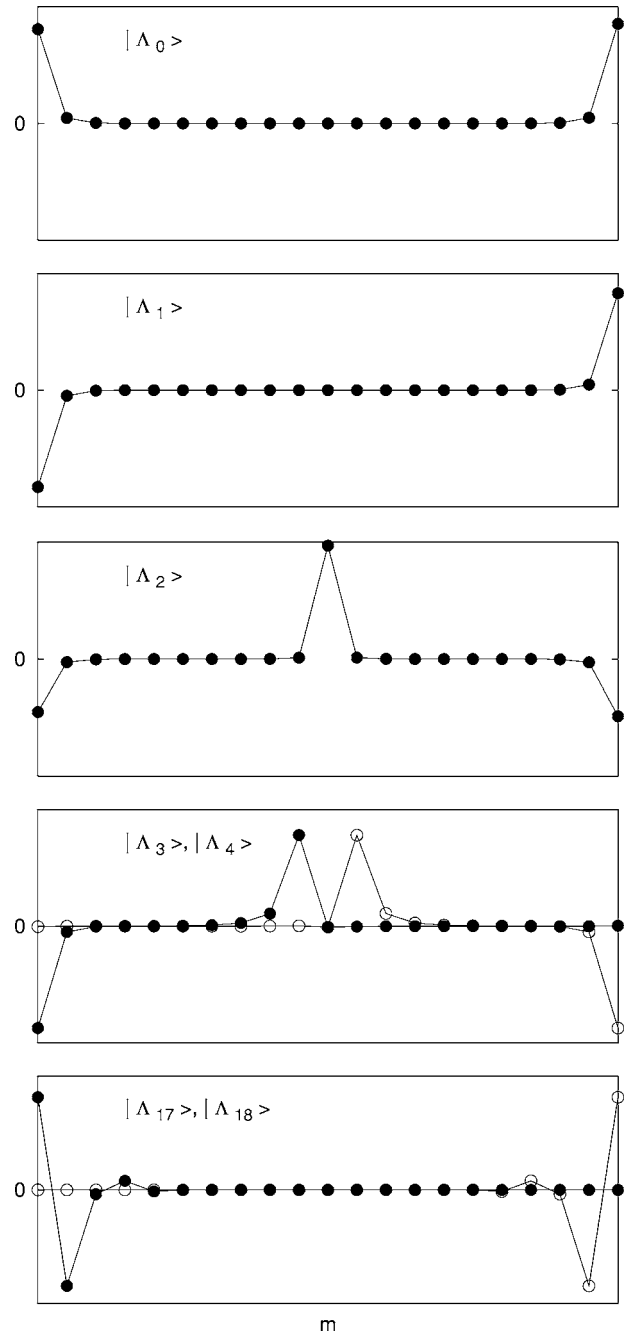


FIG. 3. Eigenvectors of the relaxation matrix \mathcal{R} for $S = 10$, $\sigma = 15$, and $\lambda = 10^{-9}$ (corresponding to the zero-field eigenvalues of Fig. 2). At $h = 0$, Λ_{2m-1} and Λ_{2m} ($m \geq 2$) are degenerated; numerical diagonalization gives even-odd eigenvectors, so we use a small $h = 10^{-3}$ to localize them in one of the wells.

Second, a connection with the classical case can be drawn. The *Fokker-Planck* limit (8) of the balance equations (2) defines a Sturm-Liouville problem.³⁶ From the corresponding theory we know that the eigenvalues of the differential operator are real and can be ordered: $\Lambda_0^{cl} \leq \Lambda_1^{cl} \leq \Lambda_2^{cl} \leq \dots$. Their corresponding eigenvectors $|\Lambda_i^{cl}\rangle$ have i nodes as a function of z ($\sim m/S$). Now, for $B_z = 0$ the problem is invariant under the transformation $z \rightarrow -z$. Then, the parity operator and the relaxation matrix can be diagonalized si-

multaneously, so that there exists a basis where the eigenstates are even or odd under $z \rightarrow -z$. Well, $|\Lambda_0^{\text{cl}}\rangle$ (the Gibbs solution) is an even function with zero nodes. Next $|\Lambda_1^{\text{cl}}\rangle$ (the overbarrier transfer) is an odd function since it has 1 node, $|\Lambda_2^{\text{cl}}\rangle$ an even function (with 2 nodes), and so on. These features are retained in the discrete ($S < \infty$) case (Fig. 3). Actually, from the degenerate states (e.g., $|\Lambda_3\rangle$ and $|\Lambda_4\rangle$) we can form the symmetrical and antisymmetrical combinations, $|\Lambda_3\rangle \pm |\Lambda_4\rangle$, fully recovering the even-odd picture just discussed.

IV. ANALYTICAL APPROACH

In general, the spin response will involve $2S$ modes [see Eqs. (11) and (14)]. However, taking into account the eigenvalue structure of Sec. III B, we can approximate the response in terms of *two* main processes: one accounting for the overbarrier transfer, with characteristic time Λ_1^{-1} , and a second one describing the intrawell dynamics with a time scale Λ_w^{-1} . The latter is a sort of *collective* mode which describes the close set of intrawell processes (Fig. 2). This motivation for the two-mode approximation is reinforced by the good results it yields in the classical limit.⁹

A. Bimodal approximation

Suppose that the relaxation can be approximated by two exponentials with normalized weights a and $1-a$,

$$\Delta M_z(t) \cong \chi_z \delta B_z [ae^{-\Lambda_1 t} + (1-a)e^{-\Lambda_w t}] \quad (15)$$

or, in the frequency domain, by

$$\frac{\chi(\Omega)}{\chi_z} \cong \frac{a}{1 + i\Omega\Lambda_1^{-1}} + \frac{1-a}{1 + i\Omega\Lambda_w^{-1}}. \quad (16)$$

This bimodal description is exact for $S=1$ ($2S=2$; see Appendix D). In general a and Λ_w are coefficients to be identified with known quantities of the problem. This can be done following the approach of Kalmykov and co-workers in the classical case.⁹ They observed that we have two unknown parameters (a and Λ_w), while $\chi(\Omega)$ can be found analytically in two limits: namely, the low- Ω and high- Ω ranges. Then, from the susceptibility in these limits, the quantities a and Λ_w in the two-mode approximation can be obtained.

The low-frequency behavior of $\chi(\Omega)$ is given by [set $\Omega = 0$ in the integrand of Eq. (14)]

$$\chi(\Omega) \cong \chi_z(1 - i\Omega\tau_{\text{int}} + \dots), \quad (17)$$

with τ_{int} the *integral relaxation time*. This is defined as the area under the magnetization relaxation curve after a sudden change δB_z in the field at $t=0$:

$$\tau_{\text{int}} \equiv \int_0^\infty dt \frac{\Delta M_z(t)}{\Delta M_z(0)}. \quad (18)$$

Next, in the high- Ω limit the susceptibility can be approximated by [expand $\Delta M_z(t)$ around $t=0$ in Eq. (14) and use $\int_0^\infty dt t^n e^{-i\Omega t} = n! / (i\Omega)^{n+1}$]:

$$\chi(\Omega) \cong \chi_z \frac{i}{\Omega \tau_{\text{ef}}}, \quad \tau_{\text{ef}}^{-1} \equiv - \left. \frac{d}{dt} \left(\frac{\Delta M_z(t)}{\Delta M_z(0)} \right) \right|_{t=0}. \quad (19)$$

Note that $1/\tau_{\text{ef}}$ is (minus) the initial slope of the relaxation curve (short times \leftrightarrow high frequencies).

On forcing the proposed formula (16) to obey the exact asymptotic equations (17) and (19), one finds $\tau_{\text{int}} = a/\Lambda_1 + (1-a)/\Lambda_w$ and $\tau_{\text{ef}}^{-1} = a\Lambda_1 + (1-a)\Lambda_w$. These equations can be solved for a and Λ_w , yielding

$$a = \frac{\tau_{\text{int}}/\tau_{\text{ef}} - 1}{\Lambda_1\tau_{\text{int}} + 1/(\Lambda_1\tau_{\text{ef}}) - 2}, \quad (20)$$

$$\Lambda_w = \tau_{\text{ef}}^{-1} \frac{1 - \Lambda_1\tau_{\text{ef}}}{1 - \Lambda_1\tau_{\text{int}}}. \quad (21)$$

This reduces the problem to the obtainment of the three characteristic times τ_{int} , Λ_1^{-1} , and τ_{ef} . Naturally, they could be expressed in terms of the relaxation eigenvalues: $\tau_{\text{int}} = \sum_i a_i / \Lambda_i$ and $\tau_{\text{ef}}^{-1} = \sum_i a_i \Lambda_i$. However, the goal is to bypass the eigenvalue (numerical) computation by calculating them directly (including Λ_1). This will result in a closed expression for the bimodal ansatz (16).

B. Calculation of τ_{int} , Λ_1 , and τ_{eff}

In the classical limit, Brown³ calculated the lowest non-vanishing eigenvalue Λ_1 in the high-barrier case, while Coffey and co-workers³¹ derived τ_{ef} ($\nabla\sigma$). On the other hand, Garanin calculated τ_{int} for a system of quantum balance equations to which Eq. (2) can be reduced. In this subsection we generalize those results for Λ_1 and τ_{ef} to the quantum case (recovering the classical formulas in the limit $S \rightarrow \infty$), and extend the result for τ_{int} to the generic system (2) of balance equations.

1. Integral relaxation time, τ_{int}

The calculation of τ_{int} is based on that the susceptibility can be calculated analytically up to first order in Ω .¹⁹ On so doing, one finds, for τ_{int} (see Appendix B),

$$\tau_{\text{int}} = \frac{\beta}{\chi_{z m=-S}} \sum_{m=-S}^S \frac{\Phi_m^2}{N_m^{(0)} P_{m+1|m}}, \quad (22)$$

where $\Phi_m = \sum_{j=-S}^m N_j^{(0)} (M_z - j)$. Notice that Φ_m only involves equilibrium averages, being independent of the spin-bath coupling model.

The dependence of $P_{m|m'}$ in the denominator on the energy differences gives *minima* in the relaxation rate at the crossing fields.³⁷ They must not be confused with the *maxima* in the rate due to tunneling.¹⁰⁻¹²

2. Lowest eigenvalue Λ_1

The calculation of Λ_1 , which corresponds to the Kramers' rate, constitutes an important task by itself. Needless to say its relevance in the theory of activated processes.^{5,6} In the *classical* case it is possible to derive an expression for Λ_1 ,³ giving good results for not too strong fields.³⁸ In the quantum case, there exists a closed analytical expression for Λ_1 only

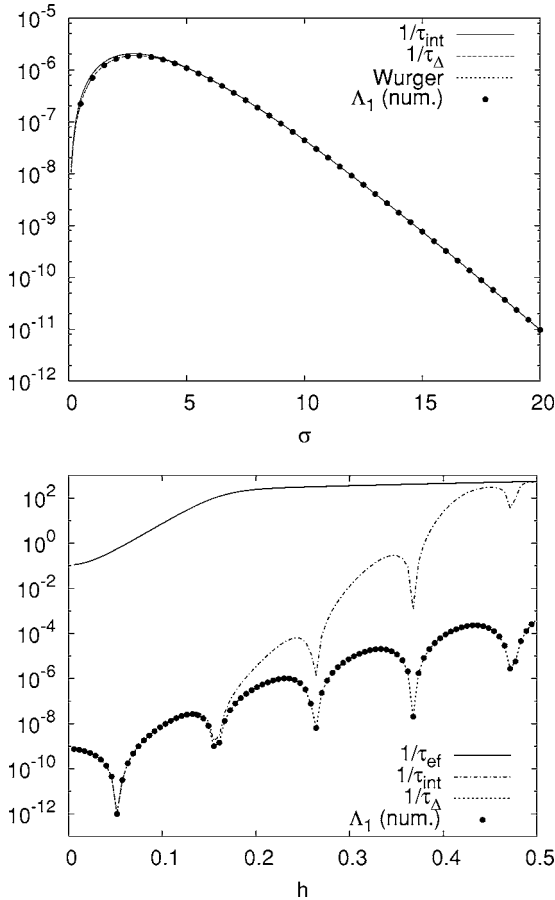


FIG. 4. Different characteristic times for a spin $S=10$ (normalized by the spin-bath coupling $\lambda=10^{-9}$). Top panel: comparison between the analytical τ_{int}^{-1} , τ_{Δ}^{-1} , and the numerical lowest eigenvalue Λ_1 in the zero-field case as a function of σ , the barrier height, for $T=0.1$. Würger’s formula [Eq. (23)] and τ_{Δ} [Eq. (25)] have a maximum relative deviation of 10^{-3} in the plotted range (at the lowest σ ’s). Bottom: τ_{int}^{-1} , τ_{Δ}^{-1} , τ_{eff}^{-1} [Eq. (27)], and Λ_1 as a function of the field for $\sigma=15$. The relative difference between τ_{Δ}^{-1} and Λ_1 never exceeds the 1% at not too strong fields ($h \leq 0.5$).

for $B_z=0$ due to Villain and co-workers,¹⁷ which was later on reexamined and improved by Würger.¹⁸ Their result can be written in a form appropriate for future comparison as

$$\Lambda_1^{-1} = \sum_{m=0}^{S-1} \frac{\theta_m}{N_m^{(0)} P_{m+1|m}}, \quad (23)$$

with $\theta_m = \sum_{j=m+1}^S N_j^{(0)}$.

Both Λ_1 from Eq. (23) and τ_{int}^{-1} from Eq. (22), together with the exact numerical eigenvalue Λ_1 are displayed in Fig. 4 showing their agreement at $B_z=0$. However, as we increase the field τ_{int}^{-1} and Λ_1 deviate from each other. This is natural; should $\tau_{\text{int}}^{-1} \cong \Lambda_1$, the response would be always described by one mode: namely, the overbarrier (i.e., $a \cong 1$ in the bimodal approximation). The same departure was found in the classical limit.^{7,8} The physical reason for the disagreement between τ_{int}^{-1} and Λ_1 is the intrawell processes entering into scene at a finite $h=B_z/D(2S-1)$. Formally, at $h \ll 1$, the quantity $\Phi_m^2/P_{m+1|m}N_m^{(0)}$ in Eq. (22) is highly peaked at the

barrier ($m=m_b$) and it is well approximated accounting only for the overbarrier process; then, $\tau_{\text{int}}^{-1} \cong \Lambda_1$. Increasing the field, however, Φ_m^2 develops a second peak around the bottom of the lower well, $m \cong S-1$, and the sum acquires a relevant contribution from the intrawell processes⁸ (see also Fig. 7 in Appendix C).

Therefore, if we want to have a closed formula under the bimodal approximation, we need to generalize the analytical expression for Λ_1 to arbitrary fields. To this end, one can seek for an observable where only overbarrier processes are reflected; then, its associated integral relaxation time may approximate well Λ_1 . This worked in the classical case, where Garanin³⁹ introduced the so-called new integral relaxation time τ_{Δ} . We will follow his steps to generalize τ_{Δ} to the quantum case, choosing as observable the difference of the well populations $\Delta \equiv N_+ - N_-$. To obtain the associated integral relaxation time, we need the low- Ω behavior of Δ , involving the “static” response $\chi_{\Delta} \sim \partial B_z \Delta$ [cf. the case of the magnetization (17)]:

$$\chi_{\Delta}(\Omega) = \frac{\partial \Delta(\Omega)}{\partial B_z} \cong \chi_{\Delta}(1 - i\Omega\tau_{\Delta} + \dots). \quad (24)$$

The calculation is carried out in Appendix B, yielding

$$\tau_{\Delta} = \frac{\beta}{\chi_{\Delta}} \sum_{m=-S}^{S-1} \frac{\Phi_m \Phi_m^N}{N_m^{(0)} P_{m+1|m}}, \quad (25)$$

with $\Phi_m = \sum_{j=-S}^m N_j^{(0)}(M_z - j)$, as before, but $\Phi_m^N = \sum_{j=-S}^m N_j^{(0)}[\Delta - \text{sgn}(j-m_b)]$. It results that $\Phi_m \Phi_m^N$ is nearly constant. Then the sum in Eq. (25) has only one main contribution (around the barrier $m \cong m_b$, due to the minima in $P_{m+1|m}$), not reflecting the dynamics inside the wells, as it was intended.

Figure 4 also shows that at zero field, τ_{Δ} matches Würger’s result (23) for Λ_1 . In fact, it can be seen analytically that our $\tau_{\Delta|_{h=0}}$ reduces in the high-barrier regime to Eq. (23) (see Appendix C). Another limit where an expression for Λ_1 is available is the classical case. Taking the limit $S \rightarrow \infty$ in τ_{Δ} we obtain, in the high barrier range ($\sigma \gg 1$),

$$\Lambda_1 \cong \pi^{-1/2} \sigma^{3/2} 2G(h) \{ (1+h) \exp[-\sigma(1+h)^2] + (1-h) \exp[-\sigma(1-h)^2] \}. \quad (26)$$

For $G(z) = (1-z^2)/2\tau_D$ (Appendix A), we recover Brown’s result for Λ_1 . Finally, in the quantum case and $h \neq 0$, we have to check τ_{Δ} with the numerical results for Λ_1^{-1} ; this is also done in Fig. 4. There we see that, in contrast to the ordinary integral relaxation time, τ_{Δ}^{-1} provides a remarkable approximation for the Kramers’ rate *at all fields*.

3. Effective time τ_{eff}

We conclude with the effective time. By definition τ_{eff} is basically the initial slope of the magnetization; see Eq. (19). Our initial condition is the system at thermal equilibrium with $B_z = B_z^0 + \delta B_z$. Then, $N_m(0)$ is known, whence $\dot{N}_m(0)$ follows directly [through Eq. (2)]. Next, $d\Delta M_z/dt|_{t=0}$ is calculated from $\dot{N}_m(0)$ (see Appendix B for details). From these one gets

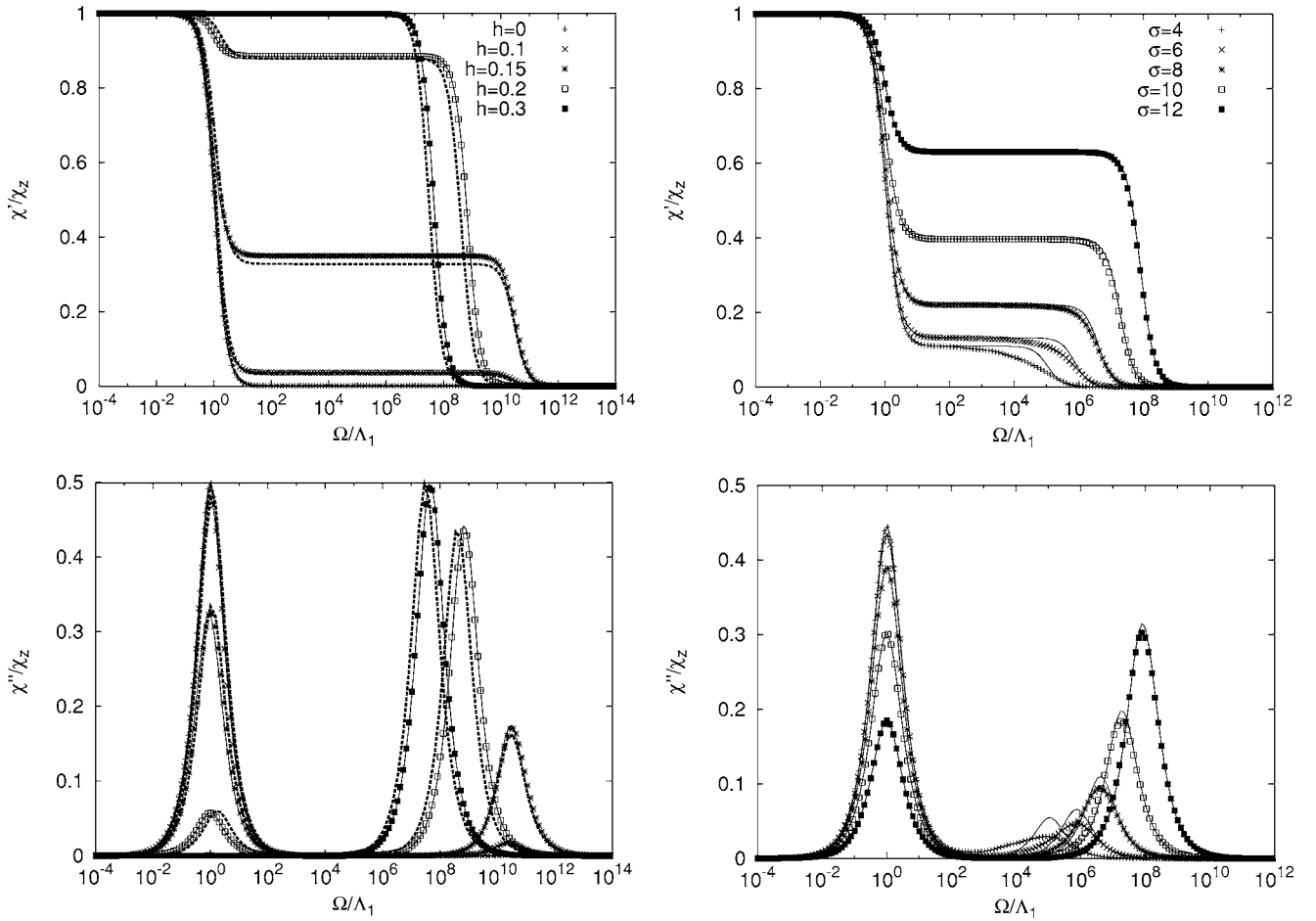


FIG. 5. Real parts (top) and imaginary parts (bottom) of the dynamical susceptibility of a spin $S=10$ with $\lambda=10^{-9}$ at $T=0.1$. The symbols represent exact numerical results and the solid lines the bimodal formula (16). Left panels: spectra at $\sigma=15$ in various applied fields $h = B_z/D(2S-1)$. The thick dashed lines are again the bimodal formula but with the simplified a , Λ_1 , and Λ_w from Eqs. (29)–(31). Right panels: spectra for a fixed field $h=0.2$ at various σ .

$$\tau_{\text{eff}}^{-1} = \frac{\beta}{\chi_{zm=-S}} \sum_{N_m^{(0)} P_{m+1|m}}, \quad (27)$$

which is the expression needed for τ_{ef}^{40}

The classical ($S \gg 1$) limits of Eqs. (22), (25), and (27) recover the expressions derived in several works from the Fokker-Planck equation (8). They are the sought analytical expressions for the characteristic times τ_{int} , Λ_1^{-1} , and τ_{eff} in the quantum case. Together with Eqs. (20) and (21) they provide a closed formula for the response under the bimodal approximation, which can be checked against exact numerical results.

V. RESULTS FOR THE DYNAMIC RESPONSE

In this section we present the full dynamical response of the spin. We compare exact numerical results with the approximate bimodal formula constructed in the previous section. We also present simplified expressions in the Kramers' regime.

The basic phenomenology is shown in Fig. 5. At weak fields the response is dominated by the overbarrier mode (the

intrawell modes are active, but by symmetry they do not contribute to the average response $\langle M_z \rangle$). Increasing the field or lowering T (raising σ) the fast modes show up in the response, leading to a peak at high frequencies.

To obtain numerically exact results for the response [see Eqs. (11)–(14)], we compute numerically all the eigenvalues Λ_i and amplitudes a_i . Comparison between them and the analytical formula (16) is shown in Fig. 5. The left panels display the susceptibility spectra in various longitudinal fields at large σ and the agreement with the bimodal approximation. The σ dependence is presented in the right panels for a fixed h . The slow dynamics at $\Omega \sim \Lambda_1$ is always captured by the formula. However, reducing sufficiently σ the bimodal approximation starts to fail at high frequencies $\Omega \sim \Lambda_w$. Specifically, the second peak in the (exact) imaginary part is no longer a single Lorentzian and a broadening with respect to the analytical curve is observed.

The reason for the overall agreement between the bimodal approximation and the exact results can be understood as follows. The overbarrier dynamics must be well captured, since it is exactly given by Λ_1 , while Λ_1 is remarkably approximated by τ_Δ (see Sec. IV). On the other hand, in the two-mode approximation we assumed that the intrawell

modes are close to one another, so that they can be described with the collective scale Λ_w .⁴¹ We have checked that their degree of closeness does not depend on σ so as to explain the disagreement for low σ and high Ω in Fig. 5. What happens is that at high σ the bimodal approximation works very well because only intrawell processes involving a few lowest well states are active, yielding $a_i \sim 0$ for the rest of the modes. In the example shown, $S=10$, one indeed sees that at $\sigma=15$, only a_{17} and a_{18} contribute [involving $m=\pm S$ and $m=\pm(S-1)$] and to a smaller extent a_{16} and a_{19} (see the inset in Fig. 2). But lowering enough the barrier, more and more intrawell modes play a role, broadening the curve. Anyway, we have to go as down as to $\sigma=6$ to find large disagreements, while most experiments in these systems are performed at $\sigma \geq 10-20$.

A. Intrawell versus overbarrier processes

Let us study in more detail the relative importance of the intrawell and overbarrier dynamics in the response, a subject that received some attention in the classical case.^{7,8} The competition between them becomes mediated by a in our Eq. (16). In particular when $a=1$ only relaxation across the barrier takes place while at $a=0$ the opposite occurs.

From Fig. 5 we learned that the relative weight of the two modes depends both on the field and the barrier height. Therefore, we need to assess the h and σ dependences of a . This is drawn in Fig. 6 for different S , along with the numerical a_1 , and the main features are as follows. Concerning the h dependence, the transition from overbarrier-dominated ($a \sim 1$) to intrawell-dominated response ($a \sim 0$) takes place in a relatively small interval of h . Second, the transition occurs at larger values of h for smaller S [approaching the classical result $h_c \approx 0.15-0.17$ (Refs. 7 and 8)]. In addition, the σ dependence of a shows that the value of S is also crucial in the low-temperature limit $\sigma \rightarrow \infty$. There a tends to 1 or to 0 depending on S .

Let us try to explain qualitatively these results, invoking a statistical mechanical argument. Inspecting the level structure of the spin Hamiltonian, we see that at $B_z = D$ the levels $-m$ and $m-1$ become degenerated. Such field corresponds to [$h = B_z/D(2S-1)$]

$$h^* \equiv \frac{1}{2S-1}. \quad (28)$$

Then, if $h < h^*$, the first excited level is $m=-S$ (in the other well), whereas if $h > h^*$, it becomes $m=S-1$ (inside the same well). At large σ it suffices to consider the fundamental state and the first excited level only. Then, when $\sigma \rightarrow \infty$, if $h < h^*$, intrawell processes are inhibited, because only $m=S$ and $m=-S$ are populated, giving $a=1$. On the contrary if $h > h^*$, the states that contribute are $m=-S$ and $m=S-1$, in the same well, so that $a=0$.

The above argument also serves to explain the large σ limits in Fig. 6, because the field used, $h=0.15$, is lower than h^* for $S=1,2,3$ and greater than h^* ($S \geq 4$). On the other hand, we have $h^* \rightarrow 0$ when $S \rightarrow \infty$. This is in agreement with the classical results⁸ where $a \rightarrow 0$ as soon as one makes $h \neq 0$ in the limit $\sigma \rightarrow \infty$. Eventually our statistical-mechanical

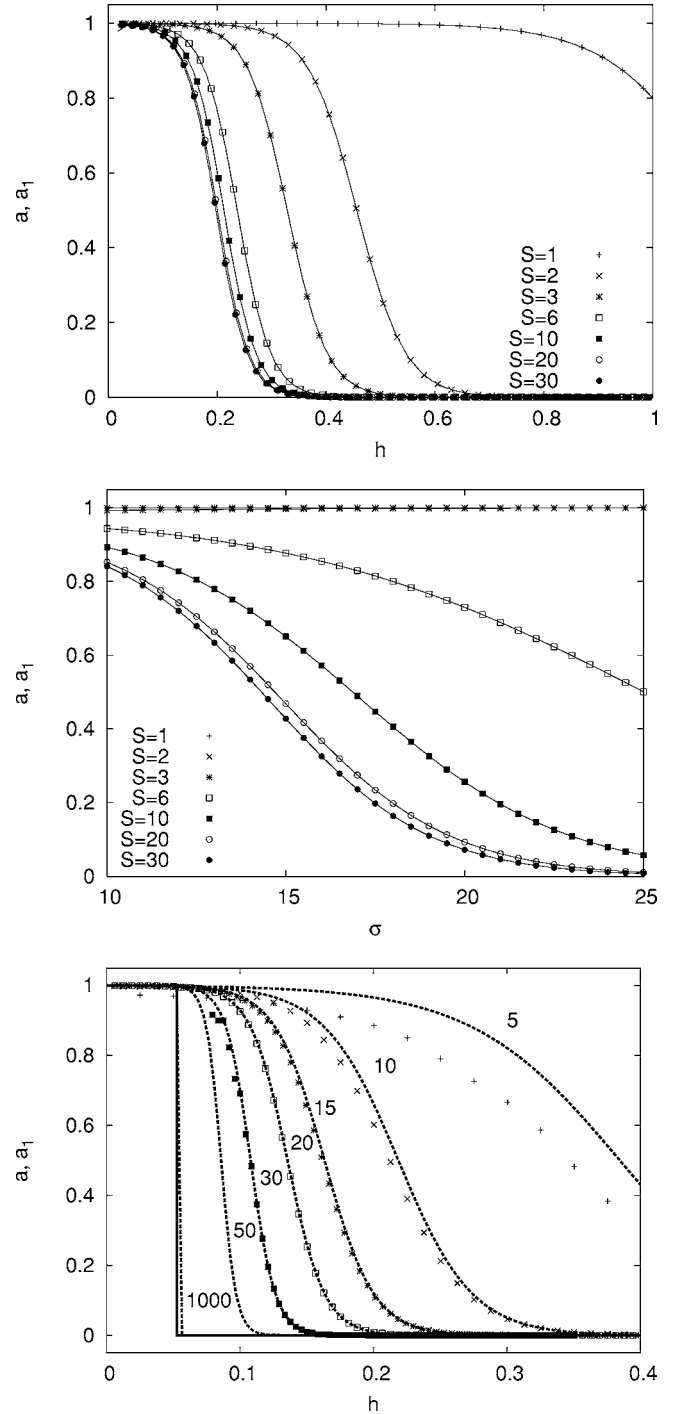


FIG. 6. Top panel: field dependence of a_1 (points) and a (lines) for different values of S . We have fixed $\sigma=15$, $\lambda=10^{-9}$, and $T=0.1$. Middle: barrier dependence of a_1 and a for the same S 's. The effective field is here fixed at $h=0.15$. Bottom: field dependence of a_1 for $S=10$ together with the approximate a of Eq. (29) for several σ (numbers by the curves). Increasing σ the curves approach a step function (solid line). At $\sigma=30$ we face numerical instabilities, so that for $\sigma=50, 1000$ only the approximate formula is plotted.

argument also explains the S dependence of the field for the onset of intrawell modes (at higher h the smaller S is). Specifically, it gives a step function $\Theta(h^*-h)$ at $\sigma \rightarrow \infty$, while the actual curves can be understood as a smoothing of such an

abrupt step due to finite temperature (Fig. 6).

B. Approximate expressions in the Kramers' regime

To conclude we present approximate formulas for the two time scales of the response, Λ_1 and Λ_w , in the high-barrier (Kramers) regime and for the parameter a controlling their relative weight. In this regime a is well described by the formula (see Appendix C)

$$a^{-1} \cong 1 + \frac{1}{4S^2} e^{\sigma(q+1)^2(h-h^*)}, \quad (29)$$

where $q=(S-1)/S$ and $h^*=1/(2S-1)$. Returning for a moment to the previous discussion, note that this formula captures the h , σ and S dependences of Fig. 6; for instance, it approaches the step function $\Theta(h-h^*)$ when $\sigma \rightarrow \infty$ and gives its smoothing for finite σ .

Let us go now into the Kramers' rate. At low temperatures Λ_1 can be expressed in terms of the barriers $\Delta U_{\pm} \equiv \varepsilon_{m_b} - \varepsilon_{\pm S}$ in a clear Arrhenius form (Appendix C)

$$\Lambda_1 \cong (e^{-\beta\Delta U_+} + e^{-\beta\Delta U_-}) \left(\frac{1}{P_{m_b+1|m_b}} + \frac{1}{P_{m_b-1|m_b}} \right)^{-1}. \quad (30)$$

Recall that the transition probabilities $P_{m|m'} = |\bar{\ell}_{m,m'}|^2 W_{m|m'}$ [Eq. (5)] involve the coupling matrix elements $\bar{\ell}_{m,m\pm 1} = (2m\pm 1)\sqrt{S(S+1)-m(m\pm 1)}$ and the rates $W_{m|m'} = \lambda \Delta_{mm'}^{\kappa} / (e^{\beta\Delta_{mm'}} - 1)$. Equation (30) generalizes the zero-field result of Villain and co-workers.¹⁷ In addition, with the appropriate $\bar{\ell}_{m,m\pm 1}$ and the spectral index κ (in $J = \lambda\omega^{\kappa}$), our formula is also applicable to other couplings and baths.

Finally we turn to the fastest mode Λ_w . In order to fix some time scale in the problem, we measure Λ_w relative to Λ_1 . Under the same assumptions used to obtain the above a and Λ_1 , we find, for Λ_w/Λ_1 ,

$$\frac{\Lambda_w}{\Lambda_1} = \frac{1}{4S^2} \frac{a}{1-a} \left(\frac{1}{P_{m_b+1|m_b}} + \frac{1}{P_{m_b-1|m_b}} \right) \times (e^{\beta\Delta U_+} P_{S-1|S} + e^{\beta\Delta U_-} P_{-S+1|-S}). \quad (31)$$

Note that Eq. (29) depends only on parameters of the spin Hamiltonian, being independent of the coupling model (as in the classical case⁸); naturally, the same holds for the barriers ΔU_{\pm} . However, the transition rates at the wells $P_{\pm(S-1)|\pm S}$ and at the barrier $P_{m_b\pm 1|m_b}$ are quite sensitive to the interaction. Thus Λ_1 or the ratio Λ_w/Λ_1 can be used to compare different couplings or baths.

Formulas (29)–(31) provide simple expressions appropriate for the experiments in the superparamagnetic range, out-of-resonance conditions. Their reasonable agreement with the exact numerical results can be seen in Fig. 5 (dashed lines). It is worth recalling that their derivation assumes that the first few levels are populated and they are therefore valid for $\sigma/S \gg 1$ (Appendix C). Then, in contrast to their exact counterparts, one cannot use Eqs. (29)–(31) to take the classical limit. Still, they result to be accurate enough down to $\sigma/S \approx 1$. Thus, they allow one to make the connection with several classical results for $\sigma \gg 1$.^{42,43}

Under resonant conditions ($\varepsilon_{-m} = \varepsilon_{m-k}$), a transverse field would induce tunneling and the balance equations lose the three-term recurrence form⁴⁴ which allowed us to derive the closed-form solutions. However, we expect that our expressions would still work after some modifications. For instance, the exponential decrease of the tunnel probability as m increases into the wells makes tunneling effective only through a few states near the top of the barrier. Then, we could try our formulas replacing m_b , not by the barrier top, but for the level at which the activated tunnel proceeds ($|m| \leq 3, 4$ in Mn_{12}).

VI. SUMMARY

The relaxation theory of a quantum superparamagnet has been developed. We have studied the minimal model: namely, a spin of arbitrary S with uniaxial anisotropy in a longitudinal field. Scarce results were available for the full dynamical response in the presence of external fields. Still, the popular single-Debye form for the susceptibility spectra could be expected to fail, in analogy with the classical situation. Here, these topics have been addressed in the frame of quantum balance equations grounded on the system-plus-bath approach to quantum dissipative systems.

We began by analyzing the eigenstructure of the relaxation matrix associated to the linear system of balance equations. The form of the eigenvectors allowed us to identify and classify the different relaxation mechanisms. In this way, full content has been given to popular statements about the relation between eigenvalues and relaxation modes. Besides, we have put it in connection with the Sturm-Liouville eigenstructure of the classical Fokker-Planck limit (parity, nodes, etc.).

Two main processes emerge: activation over the anisotropy barrier, with a time scale Λ_1^{-1} , and a bunch of close (in logarithmic scale) fast intrawell modes, with an ‘‘average’’ time scale Λ_w^{-1} . The identification and separation of the relaxation constants suggest the introduction of an approximate two-mode expression for the dynamical susceptibility. Then, following the approach of Kalmykov *et al.* in the classical case, the parameters of that formula have been expressed in terms of three characteristic quantities: integral relaxation time τ_{int} , lowest nonvanishing eigenvalue Λ_1 (Kramers' rate), and initial slope of the magnetization decay τ_{eff} . The usefulness of the classical approach stemmed from these three times being obtainable analytically (which was done over the years for different relevant situations). Then, we were left with the task of finding them all in analytical form in the quantum domain. This has been accomplished here, obtaining formulas for the quantum τ_{int} , Λ_1 (via the integral relaxation time for the population difference τ_{Δ}), and τ_{eff} , which recover the classical results when taking the $S \rightarrow \infty$ limit. With them, one has a bimodal equation for the dynamical susceptibility of a spin with arbitrary S where all ingredients can be expressed in closed form.

We have compared exact numerical results with such bimodal expression; the formula results to be quite accurate, especially in the superparamagnetic regime ($\Delta U/k_B T \sim 10-20$, the range of major experimental activity). Its limits

of validity have been assessed and interpreted in physical terms. Furthermore, in the range where the bimodal description works best, we have derived simple analytical expressions for Λ_1 , Λ_w , and a (the parameter controlling the weights of the two effective modes). These expressions generalize (quantum) formulas available at zero field and can be applied to other structures of the coupling and spectral densities of the bath (e.g., Kondo coupling to electron-hole excitations).

The onset of competence of the intrawell and overbarrier modes had been quantified to occur at $h_c \approx 0.15-0.17$ in the classical case.^{7,8} Here we have found that the equivalent quantity depends on the spin value (Fig. 6). Quantitatively, one can define $h_c(S)$ as the field making $a=1/2$. Using the approximate Eq. (29) for $a(\sigma, h, S)$ we find

$$h_c(S) \approx h^* + \frac{\ln(2S)}{2\sigma(1-1/2S)^2}, \quad (32)$$

with $h^* = 1/(2S-1) = h_c|_{\sigma \rightarrow \infty}$. Then, for the reduced barrier $\sigma=15$ (Fig. 6) we get the numbers (taking care of not leaving the validity range $\sigma/S \geq 1$) $h_c(S=1) \approx 1.1$, $h_c(2) \approx 0.4$, $h_c(3) \approx 0.3$, $h_c(6) \approx 0.2$, and $h_c(10) \approx 0.15$, approaching indeed the classical estimates.

In the presence of terms not commuting with S_z in the Hamiltonian (e.g., transverse fields) the situation is expected to be altered by tunnel events between resonant levels $-m$ and $m-k$. Then, our starting system of balance equations is no longer exact. However, in the superparamagnetic range, thermal activation is still expected to govern the physics. Actually, in nonresonant conditions (the generic case), tunneling is inhibited, while at the resonances, it can be accounted for heuristically by lowering the effective barrier a few states (Fig. 1). Thus, we hope that the two-mode picture will be of use with the appropriate amendments.

The formulas derived cover experiments even under moderate-to-strong fields, where little work had been done. The onset of competence of the dynamics inside the wells with the overbarrier mode ($h_c \sim 0.15-1$) would occur at fields of a few tesla (for Mn_{12} , $2DS \sim 10$ T), so that comparison with experimental data would be possible. The full observation of the second peak would require frequencies in the MHz to GHz range (assuming the low- Ω peak at ~ 1 Hz), but the associated raising of the real part could be detected at low frequencies. We finally remark that the treatment employed covers from the deep quantum case ($S \sim 1$) all the way up to the classical regime ($S \gg 1$). Thus, the equations derived recover, in the limit $S \rightarrow \infty$, the classical works on magnetic nanoparticles.

ACKNOWLEDGMENTS

This work was supported by DGES, Project No. BFM2002-00113, and DGA, Project PRONANOMAG, and Grant No. B059/2003. We acknowledge F. Luis, L. Martín-Moreno, and D. Prada for useful discussions and their support during this work.

APPENDIX A: CLASSICAL LIMIT OF BALANCE EQUATIONS

In this appendix we consider the classical limit of the balance equation (2). Any limit procedure requires one to specify which quantities are kept constant and which scaled variables are needed to monitor the evolution. For the classical limit, a natural choice is to maintain a fixed σ and ξ . At constant T this implies keeping the anisotropy-barrier height and amount of Zeeman energy constant. This means that the levels tend to a continuum, so $\Delta_{m,m\pm 1} \rightarrow 0$. Then we need the behavior of $P_{m|m\pm 1}$ near $\Delta_{m,m\pm 1}=0$. Expanding $P_{m|m'}$ up to first order, with $d_x f(x)|_{x=0} = -d_x f(-x)|_{x=0}$, and the detailed balance condition (3),

$$\left. \frac{dP_{m|m'}}{d\Delta_{mm'}} \right|_{\Delta_{mm'}=0} = -\beta \frac{1}{2} P_{m|m'} (\Delta_{mm'} = 0);$$

therefore,

$$P_{m|m'} = P_{m|m'}(0) - \frac{P_{m|m'}(0)}{2} \beta \Delta_{mm'} + \mathcal{O}(\beta \Delta_{mm'}^2). \quad (A1)$$

Now, it is convenient to introduce the notation

$$p_m \equiv P_{m+1|m}(0), \quad p_{m-1} \equiv P_{m|m-1}(0), \quad (A2)$$

identifying through this appendix $\Delta_{mm'} \equiv \beta \Delta_{mm'}$ and inserting Eq. (A1) into Eq. (2),

$$\begin{aligned} \dot{N}_m = & \left(p_m + \frac{p_m}{2} \Delta_{m+1,m} \right) N_{m+1} \\ & - \left(p_m - \frac{p_m}{2} \Delta_{m+1,m} \right) N_m \\ & + \left(p_{m-1} - \frac{p_{m-1}}{2} \Delta_{m,m-1} \right) N_{m-1} \\ & - \left(p_{m-1} + \frac{p_{m-1}}{2} \Delta_{m,m-1} \right) N_m, \end{aligned} \quad (A3)$$

where we have utilized Eq. (A2). Now, writing $p_{m-1} = p_m + [p_{m-1} - p_m]$ and multiplying the right-hand side of Eq. (A3) by S^2/S^2 we obtain

$$\begin{aligned} \dot{N}_m = & \frac{p_m}{S^2} [S^2(N_{m+1} - 2N_m + N_{m-1})] \\ & + \frac{p_m}{S^2} \left[S^2 \frac{1}{2} (\Delta_{m+1,m} N_{m+1} + \Delta_{m+1,m} N_m \right. \\ & \left. - \Delta_{m,m-1} N_m - \Delta_{m,m-1} N_{m-1}) \right] \\ & + S \left(\frac{p_m}{S^2} - \frac{p_{m-1}}{S^2} \right) \left[S(N_m - N_{m-1}) \right. \\ & \left. + \frac{S}{2} \Delta_{m,m-1} (N_m + N_{m-1}) \right] \end{aligned} \quad (A4)$$

In the first line of Eq. (A4) we recognize the usual discretization of the second derivative:

$$S^2(N_{m+1} - 2N_m + N_{m-1}) \rightarrow \frac{\partial^2 W(z,t)}{\partial z^2}, \quad (\text{A5})$$

where $W(z,t)$ is the classical spin distribution. The third line can be identified with the discretizations of the first derivatives:

$$\begin{aligned} S(N_m - N_{m-1}) &\rightarrow \frac{\partial W(z,t)}{\partial z}, \\ S\Delta_{m+1,m} = \beta S(\varepsilon_{m+1} - \varepsilon_m) &\rightarrow \frac{\partial u(z)}{\partial z}, \\ S\left(\frac{p_{m+1}}{S^2} - \frac{p_m}{S^2}\right) &\rightarrow \frac{\partial G(z)}{\partial z}; \end{aligned} \quad (\text{A6})$$

here, we have utilized that $p_m/S^2 \rightarrow G(z)$. The function $G(z)$ depends on the specific form of p_m [$\equiv P_{m+1|m}(0)$] and $u(z)$ is the classical energy function [$u(z) \equiv \beta \mathcal{H}(z)$]. Finally, the second line is the discretization of $\frac{\partial}{\partial z} \left(\frac{\partial u(z)}{\partial z} \right) W(z,t)$, since

$$\begin{aligned} S^2 \frac{1}{2} (\Delta_{m+1,m} N_{m+1} + \Delta_{m+1,m} N_m - \Delta_{m,m-1} N_m - \Delta_{m,m-1} N_{m-1}) \\ \rightarrow \frac{\partial}{\partial z} \left(\frac{\partial u(z)}{\partial z} \right) W(z,t). \end{aligned} \quad (\text{A7})$$

Using Eqs. (A5)–(A7), we obtain the continuum version of Eq. (2), Eq. (8), where $G(z) \equiv P_{m+1|m}(0)/S^2$. Let us emphasize that this derivation only makes use of detailed balance condition (3), and a nonvanishing transition probability at zero frequency $P_{m+1|m}(0)$, which has been tacitly assumed from the beginning.

In this problem (no transversal field, rotating-wave approximation) we could take advantage of the system of balance equations to take the classical limit directly in terms of the N_m . On the other hand, when the off-diagonal density matrix elements need to be considered, taking the classical limit requires a spin coherent state representation (phase space) for the density matrix.⁴⁵

We conclude making the connection with Brown's classical theory.³ It starts from a Landau-Lifshitz equation describing the precession of the magnetic moment: $\gamma^{-1} d\vec{m}/dt = \vec{m} \times (\vec{B} + \vec{b}) - (\lambda_{LL}/m) \vec{m} \times (\vec{m} \times \vec{B})$, with λ_{LL} the damping constant and $\vec{b}(t)$ a fluctuating field. This is assumed with isotropic statistical properties and white noise spectrum. In the absence of transverse fields this Langevin equation corresponds to the Fokker-Planck equation (8) with $G(z) = (1 - z^2)/2\tau_D$ and $\tau_D^{-1} = \lambda_{LL}/2\beta(m/\gamma)$. (For the comparison below, recall that the magnetic moment over the gyromagnetic ratio m/γ corresponds to the spin value S .)

To recover this theory from the spin-plus-bath formulation, we consider an Ohmic bath $J(\omega) = \lambda\omega$ (corresponding to the white noise assumption), a linear coupling $F = \frac{1}{2}(\eta_+ S_- + \eta_- S_+)$ (corresponding to field-like fluctuations), where in the parameters incorporating the symmetry of the coupling, $\eta_{\pm} = \eta_x \pm i\eta_y$; we set $\eta_x = \eta_y = 1$ (i.e., isotropic fluctuations). Then, from the coupling matrix elements $\ell_{m,m\pm 1}$

$= \sqrt{S(S+1) - m(m\pm 1)}$ and Ohmic rate function $W(\Delta) = \lambda\Delta/(e^{\beta\Delta} - 1)$ (see Sec. II B), one finds $G(z) = P_{m+1|m}(0)/S^2 = (\lambda/2\beta)(1 - z^2)$. Thus, comparing with τ_D and indentifying

$$\lambda = \lambda_{LL}/2S, \quad (\text{A8})$$

we make the connection with the quantities entering in Brown's classical model. Finally, if we had considered a coupling $F(S) \propto (S_z S_{\pm} + S_{\pm} S_z)$, as the one used in the main text to deal with phonons, its classical limit [including two-phonon processes to ensure $P_{m|m\pm 1}(0) \neq 0$] would involve $G(z) \propto z^2(1 - z^2)$.

APPENDIX B: DETAILS FOR THE CALCULATION OF

τ_{int} , τ_{Δ} , AND τ_{eff}

Here we calculate the three time constants τ_{int} , τ_{Δ} , and τ_{eff} , which characterize the magnetization relaxation in the bimodal approximation (see Sec. IV).

1. τ_{int}

As τ_{int} describes the low- Ω behavior of the susceptibility our purpose here is to obtain $\chi(\Omega)$ up to first order in Ω [see Eq. (17)]. For future convenience, we write N_m as

$$N_m \equiv N_m^{(0)} + N_m^{(1)} = N_m^{(0)}(1 + \beta q_m), \quad (\text{B1})$$

where $N_m^{(0)}$ and $N_m^{(1)}$ are the zero- and first-order (in δB_z) parts of the evolution for N_m . Inserting (B1) into Eq. (2) we obtain the set of equations necessary to calculate the response in linear approximation:

$$\begin{aligned} P_{m+1|m} - P_{m-1|m} &= i\Omega q_m + P_{m+1|m}(q_{m+1} - q_m) \\ &\quad + P_{m-1|m}(q_{m-1} - q_m); \end{aligned} \quad (\text{B2})$$

here, $P_{m|m'} \equiv P_{m|m'}(B_z = B_z^0)$. To write Eq. (B2) in terms of $P_{m+1|m}$ and $P_{m-1|m}$ the detailed balance equation (3) and the equality $e^{\Delta_{m',m}} N_{m'}^{(0)} = N_m^{(0)}$ have been utilized.

We are interested in the low-frequency behavior, so we expand

$$q_m(\Omega) \equiv q_m^{(0)} + \Omega q_m^{(1)}. \quad (\text{B3})$$

We substitute (B3) into Eq. (B2), and we solve it perturbatively in Ω . The zero-frequency order gives

$$P_{m+1|m} - P_{m-1|m} = P_{m+1|m}(q_{m+1}^{(0)} - q_m^{(0)}) + P_{m-1|m}(q_{m-1}^{(0)} - q_m^{(0)}). \quad (\text{B4})$$

Since Eq. (B4) depends only on the differences $q_{m+1}^{(0)} - q_m^{(0)}$ and defining

$$\bar{q}_m \equiv q_{m+1}^{(0)} - q_m^{(0)}, \quad (\text{B5})$$

Eq. (B4) can be cast in a two-term recurrence. With the "boundary" condition $P_{-S-1|-S} = 0$ the solution reads

$$\bar{q}_m = 1 \quad (\text{B6})$$

and accordingly to (B5) and (B6),

$$q_m^{(0)} = m - M_z, \quad (\text{B7})$$

where M_z is the magnetization. To obtain Eq. (B7) the normalization condition

$$\sum_{m=-S}^S N_m^{(0)} q_m^{(0)} = 0 \quad (\text{B8})$$

has been used. The above condition comes from $\sum_m N_m^{(1)} = 0$. Besides this follows from the unicity of the Fourier expansion of the norm and $\sum_m N_m^{(0)} = 1$ plus $\sum_m N_m = 1$. Now, we write Eq. (B2) up to first order in Ω ,

$$0 = i\Omega q_m^{(0)} + P_{m+1|m}(q_{m+1}^{(1)} - q_m^{(1)}) + P_{m-1|m}(q_{m-1}^{(1)} - q_m^{(1)}). \quad (\text{B9})$$

Once more, Eq. (B4) depends only on the differences. Introducing

$$r_m \equiv P_{m+1|m} e^{-\beta \varepsilon_m} (q_{m+1}^{(1)} - q_m^{(1)}), \quad (\text{B10})$$

Eq. (B9) transforms onto a two-term recurrence relation, obtaining for the r_m elements,

$$r_m = -i\Omega \sum_{j=-S}^m q_j^{(0)} e^{-\beta \varepsilon_j}, \quad (\text{B11})$$

where we have again invoked $P_{-S-1|-S} = 0$. Now, Eq. (B11) with (B10) and the first- Ω -order normalization condition

$$\sum_{m=-S}^S N_m^{(0)} q_m^{(1)} = 0 \quad (\text{B12})$$

permit us to write $q_m^{(1)}$ as

$$i q_m^{(1)} = \sum_{i=-S}^{m-1} \frac{\Phi_i}{P_{i+1|i} N_i^{(0)}} - \sum_{j=-S}^S N_j^{(0)} \sum_{i=-S}^{j-1} \frac{\Phi_i}{P_{i+1|i} N_i^{(0)}}, \quad (\text{B13})$$

where the auxiliary function Φ_i is given by

$$\Phi_m = \sum_{j=-S}^m (M_z - j) N_j^{(0)}. \quad (\text{B14})$$

The low- Ω expansion (17) and (B1) allows to express τ_{int} as

$$i \tau_{\text{int}} = \frac{\beta}{\chi_z} \sum_{m=-S}^S m N_m^{(0)} q_m^{(1)}. \quad (\text{B15})$$

Introducing Eq. (B13) in Eq. (B15) and using the equalities

$$\sum_{j=-S}^S N_j^{(0)} \sum_{i=-S}^{j-1} \frac{\Phi_i}{P_{i+1|i} N_i^{(0)}} = \sum_{i=-S}^{S-1} \frac{\Phi_i}{P_{i+1|i} N_i^{(0)}} \sum_{j=i+1}^S N_j^{(0)} \quad (\text{B16})$$

and

$$-M_z \sum_{j=i+1}^S N_j^{(0)} + \sum_{j=i+1}^S j N_j^{(0)} = \Phi_i, \quad (\text{B17})$$

we finally obtain the formula (22) for the integral relaxation time.

2. τ_Δ

The time constant τ_Δ arises when instead of the magnetization susceptibility, one considers the low- Ω response of the difference of the well populations Δ :

$$\Delta \equiv N_+ - N_- = \sum_{m=-S}^S \text{sgn}(m - m_b) N_m, \quad (\text{B18})$$

with ε_{m_b} the maximum level. Notice that the derivation of τ_Δ must follow the same steps that for the derivation of τ_{int} . Further, taking into account the definition of Δ and from the low- Ω expansion for $\chi_\Delta(\Omega)$ [see Eq. (24)], τ_Δ is given in terms of $q_m^{(1)}$, Eq. (B13), as

$$i \tau_\Delta = \frac{1}{\chi_\Delta} \sum_{m=-S}^S \text{sgn}(m - m_b) N_m^{(0)} q_m^{(1)}. \quad (\text{B19})$$

Finally, using equalities (B16) and

$$-\Delta \sum_{j=i+1}^S N_j^{(0)} + \sum_{j=i+1}^S \text{sgn}(m - m_b) N_j^{(0)} = \Phi_j^N, \quad (\text{B20})$$

where Φ_j^N is defined as

$$\Phi_m^N = \sum_{j=-S}^m N_j^{(0)} [\Delta - \text{sgn}(j - m_b)], \quad (\text{B21})$$

formula (25) is readily obtained.

3. τ_{eff}

First we notice that the definition for τ_{eff} Eq. (19) can be rewritten in terms of $N_m(t)$ as

$$\tau_{\text{eff}}^{-1} = -\frac{1}{\Delta M_z(0)} \sum_{m=-S}^S m \dot{N}_m(0). \quad (\text{B22})$$

$\dot{N}_m(0)$ is obtained directly from the balance equation making $t=0$ in Eq. (2). Now, we recall that the system is initially at equilibrium with field $B_z = B_z^0 + \delta B_z$. Up to first order in δB_z this can be written

$$N_m(0) = N_m^{(0)} + \delta B_z \beta N_m^{(0)} (m - M_z). \quad (\text{B23})$$

Next, we insert Eq. (B23) into Eq. (2). Considering

$$P_{m|m\pm 1} N_{m\pm 1}^{(0)} = P_{m\pm 1|m} N_m^{(0)}, \quad (\text{B24})$$

Eq. (B22) reads

$$\tau_{\text{eff}}^{-1} = \frac{\beta}{\chi_z} \left(\sum_{m=-S}^S m P_{m|m-1} N_{m-1}^{(0)} - \sum_{m=-S}^S m P_{m+1|m} N_m^{(0)} \right). \quad (\text{B25})$$

Finally, performing the change $m \rightarrow m+1$ in the first summand we obtain the final formula (27) for the inverse of the effective time.

APPENDIX C: APPROXIMATE FORMULAS IN THE HIGH-BARRIER CASE

Here we derive approximate expressions for a , Λ_1 , and Λ_w in the high-barrier case.

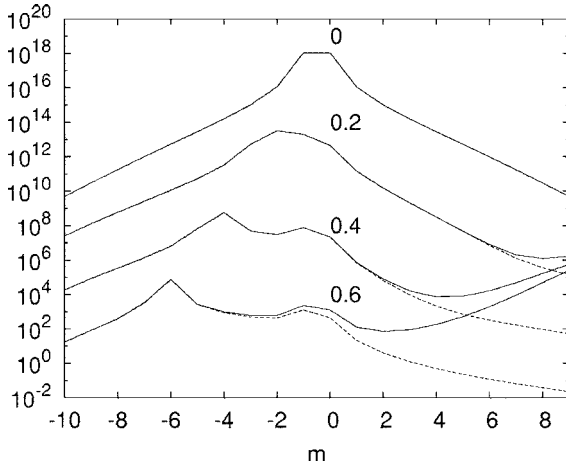


FIG. 7. Summands of τ_{int} Eq. (22), $\Phi_m^2/N_m^{(0)}P_{m+1|m}$ (solid line), and τ_{Δ} , Eq. (25), $S\Phi_m\Phi_m^N/N_m^{(0)}P_{m+1|m}$ (dashed line). Different h are drawn: $h=0,0.2,0.4,0.6$. The rest of parameters are $S=10$, $\sigma=15$, and $\lambda=10^{-9}$.

The technical difficulties deal mainly with the calculation of the sums in τ_{int} , τ_{Δ} , and τ_{eff} . For that let us first consider the main approximation to handle with Φ_m^2 and $\Phi_m\Phi_m^N$. In the range considered Φ_m can be well approximated by

$$\Phi_m \cong \Phi_B, \quad m < S-2,$$

$$\Phi_m \cong \Phi_B + \Phi_W, \quad m \cong S-1, \quad (\text{C1})$$

where $\Phi_B \cong \sum_{j=-S}^{m_b} (M_z - j)N_j^{(0)} = \Phi_{m_b}$ and $\Phi_W \cong \sum_{j=m_b+1}^{S-1} (M_z - j)N_j^{(0)} = \Phi_{S-1} - \Phi_{m_b}$. Besides there are two main contributions in the sum for τ_{int} , one around m_b and the other one around $m \cong S-1$ (see Fig. 7). This last peak in the sum is due to Φ_W . On the other hand, the quantity $\Phi_m\Phi_m^N$ results in being well approximated for practical purposes by the constant

$$\Phi_m\Phi_m^N \cong \Phi_B\Phi^N, \quad (\text{C2})$$

with $\Phi^N = \sum_{j=-S}^{m_b} (\Delta+1)N_j^{(0)} = \Phi_{m_b}^N$. Then the sum for τ_{Δ} has only one main contribution around m_b (see Fig. 7).

Now, we give the main steps to calculate the formula (29) for a . In the bimodal approximation $\tau_{\text{int}} \cong a/\Lambda_1 + (1-a)/\Lambda_w$. Then, and taking into account that $\Lambda_w \gg \Lambda_1$ and $\Lambda_1 \cong \tau_{\Delta}$,

$$a \cong \frac{\tau_{\text{int}}}{\tau_{\Delta}}. \quad (\text{C3})$$

Next we use approximations (C1) and (C2). Neglecting the second peak in the sum, which is produced by intrawell dynamics [it would contribute to the summand $(1-a)/\Lambda_w$], we write

$$a \cong S \frac{\chi_{\Delta}}{\chi_z}, \quad (\text{C4})$$

here, we have also used that in the high-barrier limit $\Phi^B = S\Phi^N$ (see Fig. 7). Notice that (C4) depends only on equilibrium magnitudes. To compute χ_z and χ_{Δ} we approximate the partition function by

$$\mathcal{Z} \cong e^{\sigma} \{ 2 \cosh \xi + e^{\sigma(q^2-1)} \cosh q\xi \}, \quad (\text{C5})$$

with $q=(S-1)/S$. This form for \mathcal{Z} has been calculated considering only the states $m=\pm S$ and $m=\pm(S-1)$. Restricting ourselves to the lowest states becomes justified when $\sigma \gg 1$. However, at sufficiently high h , levels in the right well with $m < S-1$ have less energy than $m=-S+1$ even $m=-S$; then, they would be more populated. On the other hand, this is the minimal model which includes sufficient states to deal with intrawell and overbarrier contributions. Then, from (C5) we obtain χ_z and χ_{Δ} . Finally, considering only the leading terms in σ we obtain the final expression (29) for a .

Now we turn our attention to Λ_1 . In the main text we have argued that $\Lambda_1 \cong \tau_{\Delta}^{-1}$. Then, and considering (C2), we write

$$\Lambda_1^{-1} \cong \tau_{\Delta} \cong \frac{\beta}{\chi_{\Delta}} \Phi \Phi^N \sum_{m=-S}^{S-1} \frac{1}{N_m^{(0)} P_{m+1|m}}. \quad (\text{C6})$$

We use now θ_m [see Eq. (23)]—i.e., $\theta_m = \sum_{j=m+1}^S N_j^{(0)}$; then, it can be checked that

$$\Delta \cong 2\theta_{m_b} - 1 \quad (\text{C7})$$

and

$$\chi_{\Delta} \cong 2\partial_{B_z} \theta_{m_b} = 2\beta\Phi^B. \quad (\text{C8})$$

Thus Λ_1^{-1} reads:

$$\Lambda_1^{-1} \cong (1 - \theta_{m_b}) \theta_{m_b} \sum_{m=-S}^{S-1} \frac{1}{N_m^{(0)} P_{m+1|m}}. \quad (\text{C9})$$

First, Eq. (C9) equals the Würger result (23), since $\theta_m \cong \theta_{m_b} = 1/2$. Furthermore, the sums for θ_{m_b} and $\sum 1/N_m^{(0)} P_{m+1|m}$ can be evaluated following Garanin in some limiting cases.¹⁹ In particular the classical limit can be carried out. In this limit the sum is converted into an integral, which in turn can be solved. Then using approximate expressions for the classical \mathcal{Z} when $\sigma \gg 1$ (see Sec. II of Ref. 46) and the same for θ_{m_b} , we recover the Brown result (26) for $G(z) \propto (1-z^2)$ [see Eq. (8)]. Eventually, one also considers $\sigma/S > 1$ to evaluate the sums in (C9). In this case, it becomes sufficient consider only the two main terms in the sum: namely, $1/N_m^{(0)} P_{m_b+1|m_b}$ and $1/N_m^{(0)} P_{m_b-1|m_b}$. In addition we only take into account the leading terms in σ for θ_{m_b} , obtaining the Arrhenius formula (30) for Λ_1 .

Finally we consider Λ_w . In the expression for Λ_w [Eq. (21)], the denominator can be approximated by $\Lambda_1 \tau_{\text{int}} - 1 \cong a - 1$ [see Eq. (C3)]. Finally assuming $\tau_{\text{eff}}^{-1} \gg \Lambda_1$ (see Fig. 4) Λ_w reads

$$\Lambda_w \cong \frac{\tau_{\text{eff}}^{-1}}{1-a}. \quad (\text{C10})$$

Then,

$$\frac{\Lambda_w}{\Lambda_1} = \frac{1}{4S^2} \frac{a}{1-a} \left(\sum_{m=-S}^{S-1} N_m^{(0)} P_{m+1|m} \right) \left(\sum_{m=-S}^{S-1} \frac{1}{N_m^{(0)} P_{m+1|m}} \right). \quad (\text{C11})$$

To obtain this formula we have used Eq. (C6) for Λ_1 and Eq. (C4) for a together with $\Phi_B \equiv S\Phi^N$. Now, taking only leading terms in the sum we readily obtain (31) in the regime of interest.

APPENDIX D: EXACT ANALYTICAL SUSCEPTIBILITY FOR $S=1$

When $S=1$ it is possible to derive an exact analytical expression for $\chi(\Omega)$. For that, we calculate the eigenvalues

of the, in this case, 3×3 relaxation matrix \mathcal{R} , obtaining

$$\Lambda_{1,2} = (\Gamma_+ + \Gamma_-) \mp \sqrt{(\Gamma_+ - \Gamma_-)^2 + 4P_{1|0}^{(0)}P_{-1|0}^{(0)}}, \quad (\text{D1})$$

plus the zero eigenvalue $\Lambda_0=0$. Here $\Gamma_{\pm} \equiv P_{\pm 1|0}[\mathbb{1} + \exp\{\beta(\varepsilon_{\pm 1} - \varepsilon_0)\}]$. Notice that the bimodal description is exact for $S=1$ ($\Lambda_w \equiv \Lambda_2$). Besides, using the general relation of τ_{eff}^{-1} with the eigenvalues, $\tau_{\text{eff}}^{-1} = \sum_i a_i \Lambda_i$ —i.e., $\tau_{\text{eff}}^{-1} = a\Lambda_1 + (1-a)\Lambda_2$ — a reads

$$a = \frac{\Lambda_2 - \tau_{\text{eff}}^{-1}}{\Lambda_2 - \Lambda_1}, \quad (\text{D2})$$

with $\tau_{\text{eff}}^{-1} = \beta/(\chi_z \mathcal{Z})(P_{1|0}^{(0)} + P_{-1|0}^{(0)})$.

The two modes Λ_1 and Λ_2 and a are introduced into Eq. (16) obtaining the exact expression for the response.

- ¹Q. A. Pankhurst and R. J. Pollard, *J. Phys.: Condens. Matter* **5**, 8487 (1993).
- ²L. Néel, *Ann. Geophys. (C.N.R.S.)* **5**, 99 (1949).
- ³W. F. Brown, Jr., *Phys. Rev.* **130**, 1677 (1963).
- ⁴S. J. Blundell and F. L. Pratt, *J. Phys.: Condens. Matter* **16**, R771 (2004).
- ⁵P. Hänggi, P. Talkner, and M. Borkovec, *Rev. Mod. Phys.* **62**, 251 (1990).
- ⁶V. I. Mel'nikov, *Phys. Rep.* **209**, 1 (1991).
- ⁷W. T. Coffey, D. S. F. Crothers, Y. P. Kalmykov, and J. T. Waldrom, *Phys. Rev. B* **51**, 15947 (1995).
- ⁸D. A. Garanin, *Phys. Rev. E* **54**, 3250 (1996).
- ⁹Y. P. Kalmykov, W. T. Coffey, and S. V. Titov, *J. Magn. Magn. Mater.* **265**, 44 (2003).
- ¹⁰J. R. Friedman, M. P. Sarachik, J. Tejada, and R. Ziolo, *Phys. Rev. Lett.* **76**, 3830 (1996).
- ¹¹J. M. Hernández, X. X. Zhang, F. Luis, J. Bartolomé, J. Tejada, and R. Ziolo, *Europhys. Lett.* **35**, 301 (1996).
- ¹²L. Thomas, F. Lioni, R. Ballou, D. Gatteschi, R. Sessoli, and B. Barbara, *Nature (London)* **383**, 145 (1996).
- ¹³F. Hartmann-Boutron, P. Politi, and J. Villain, *Int. J. Mod. Phys. B* **10**, 2577 (1996).
- ¹⁴D. A. Garanin and E. M. Chudnovsky, *Phys. Rev. B* **56**, 11102 (1997).
- ¹⁵F. Luis, J. Bartolomé, and J. F. Fernández, *Phys. Rev. B* **57**, 505 (1998).
- ¹⁶A. Würger, *J. Phys.: Condens. Matter* **10**, 10075 (1998).
- ¹⁷J. Villain, F. Hartmann-Boutron, R. Sessoli, and A. Rettori, *Europhys. Lett.* **27**, 159 (1994).
- ¹⁸A. Würger, *Phys. Rev. Lett.* **81**, 212 (1998).
- ¹⁹D. A. Garanin, *Phys. Rev. E* **55**, 2569 (1997).
- ²⁰The sources of magnetic anisotropy can be the interactions of the cluster spins with their neighbors' electric fields (magnetocrystalline anisotropy), dipole-dipole interactions inside the cluster (magnetostatic or "shape" anisotropy), spins at the cluster boundaries (surface anisotropy), etc.
- ²¹The maximum level is given by $m_b = -B_z/2D + F$, with $F = \mathcal{F}[B_z/2D + S + 1/2] - 1/2$ and $\mathcal{F}[x]$, the fractional part of x .
- ²²G. E. Pake and T. L. Estle, *The Physical Principles of Electron Paramagnetic Resonance*, 2nd ed. (Benjamin, Reading, MA, 1973).
- ²³N. G. Van Kampen, *Stochastic Processes in Physics and Chemistry*, 2nd ed. (North-Holland, Amsterdam, 1997).
- ²⁴H. M. Cataldo, *Physica A* **165**, 249 (1990).
- ²⁵J. L. García-Palacios and D. Zueco, cond-mat/0603730 (unpublished).
- ²⁶Then one does not need the "coherences" (off-diagonal elements) when computing observables expressible in terms of ρ_{mm} only, e.g., $\langle S_z \rangle$, $\langle S_+ S_- \rangle$, etc.
- ²⁷K. Blum, *Density Matrix Theory and Applications*, 2nd ed. (Plenum, New York, 1996).
- ²⁸The rate function $W(\Delta)$ is the Fourier-Laplace transform of the memory kernel in the original density-matrix equation $\mathcal{K}(\tau) = \int_0^\infty (d\omega/\pi) J(\omega) [n_\omega e^{+i\omega\tau} + (n_\omega + 1)e^{-i\omega\tau}]$, where $n_\omega = 1/(e^{\beta\omega} - 1)$ is the Bose factor. Neglecting imaginary parts and using $\text{Re}[\int_0^\infty d\tau e^{-i\Delta\tau}] = \pi\delta(\Delta)$ one has $W(\Delta) = \text{Re}[\int_0^\infty d\tau \mathcal{K}(\tau) e^{-i\Delta\tau}] \sim J(\Delta)n_\Delta$. For odd $J(\Delta)$, as in a Ohmic bath ($\kappa=1$) or in the $\kappa=3$ super-Ohmic bath, the result is valid irrespective of the sign of Δ (Ref. 25). Then Eq. (6) follows, which incidentally obeys detailed balance.
- ²⁹U. Weiss, *Quantum Dissipative Systems* (World Scientific, Singapore, 1993).
- ³⁰To compute $J(\omega) \sim \sum_q |V_q|^2 \delta(\omega - \omega_q)$, one uses a Debye phonon model $\omega_q \rightarrow \omega_{ks} = c_s |k|$ and replace $\sum_q \rightarrow \sum_s \int d^D k$, integrating over wave vectors and summing over branch indices. For couplings $|V_q|^2 \sim \omega_q$, one has $d^D k \times |V_{ks}|^2 \sim |k|^{D-1} \times |k|$, giving spectral densities $J \propto \omega^\kappa$, evolving from Ohmic ($\kappa=1$) for phonons in one dimension, to super-Ohmic $J \propto \omega^3$ for $D=3$.
- ³¹W. T. Coffey, P. J. Cregg, and Y. P. Kalmykov, *Adv. Chem. Phys.* **83**, 263 (1993).
- ³²S. Dattagupta, *Relaxation Phenomena in Condensed Matter Physics* (Academic, Orlando, FL, 1987).
- ³³The $|\Lambda_i\rangle$, or \mathbf{N} , are not vectors in a Hilbert space, but n -tuples ($n=2S+1$) comprising the diagonal elements of the density matrix.
- ³⁴E. Anderson *et al.*, *LAPACK User's Guide* (SIAM, Philadelphia, 1995).
- ³⁵For S half-integer, at $h=0$ the $(2S+1)$ states are double degenerated: $|\Lambda_0\rangle = |\Lambda_1\rangle = 0$ ($P_{-1/2|1/2} = 0$). The rest of eigenvalues describe symmetrical processes in both wells analogous to the ones explained for S integer.
- ³⁶G. Arfken, *Mathematical Methods for Physicists*, 3rd ed. (Academic Press, Boston, 1985).
- ³⁷At $h=(2n+1)/(2S-1)$ the lowest eigenvalue goes to zero. At these bias $m=-n$ and $m=-n+1$ become degenerate; thus, the

relaxation time diverges, since $P_{-n|-n+1}(0)=0$ in the model used.

³⁸A. Aharoni, Phys. Rev. **177**, 793 (1969).

³⁹D. A. Garanin, Europhys. Lett. **48**, 486 (1999).

⁴⁰In contrast with the other time constants, τ_{eff} has the structure of an equilibrium average (of an operator with diagonal matrix elements $P_{m+1|m}$). Then in the classical limit [for an Ohmic bath and linear coupling $F(\vec{S})$; see Appendix A], one uses $P_{m+1|m}/S^2 \rightarrow 1-z^2$ and recovers the equilibrium average form $\tau_{\text{eff}}^{-1} \sim 1-\langle z^2 \rangle$ of the classical case (Ref. 31).

⁴¹Using the sum rule $\sum_{i=1}^{2S} a_i = 1$, together with the expressions $\tau_{\text{int}} = \sum_i a_i / \Lambda_i$ and $\tau_{\text{eff}}^{-1} = \sum_i a_i \Lambda_i$, one gets, from Eq. (21),

$$\Lambda_w = \frac{\sum_{i \geq 2} a_i (\Lambda_1 - \Lambda_i)}{\sum_{i \geq 2} a_i (\Lambda_1 / \Lambda_i - 1)} \stackrel{\Lambda_1 \ll \Lambda_i}{\simeq} \frac{\sum_{i \geq 2} a_i \Lambda_i}{\sum_{i \geq 2} a_i}.$$

Thus, Λ_w is indeed an average over the fast modes when these are well separated from the overbarrier rate.

⁴²For instance, Storonkin's bimodal formula (Ref. 43), derived rigorously for zero field and $\sigma \gg 1$, involves $\Lambda_w \simeq 2\lambda_{\text{LL}} B_a$, with λ_{LL} the Landau-Lifshitz damping and B_a the anisotropy field [the same follows from Garanin's heuristic expression (Ref. 8) at $h \rightarrow 0$]. Using an Ohmic bath and a linear coupling $F(\vec{S})$ (see Appendix A), we find from Eqs. (29)–(31) that $\Lambda_w \simeq 2\lambda_{\text{LL}} \Delta_{S,S-1}$. As the ground-state splitting $\Delta_{S,S-1} = \epsilon_S - \epsilon_{S-1}$ corresponds to B_a , identifying $2S\lambda \rightarrow \lambda_{\text{LL}}$ [Eq. (A8) in Appendix A] we make the connection with Storonkin's classical results.

⁴³B. A. Storonkin, Kristallografiya **30**, 841 (1985) [Sov. Phys. Crystallogr. **30**, 489 (1985)].

⁴⁴M. N. Leuenger and D. Loss, Phys. Rev. B **61**, 1286 (2000).

⁴⁵Y. Takahashi and F. Shibata, J. Phys. Soc. Jpn. **38**, 656 (1975).

⁴⁶J. L. García-Palacios, Adv. Chem. Phys. **112**, 1 (2000).